Energy-dependent cyclotron mass in InAs/AlSb quantum wells

C Gauer†, J Scriba†, A Wixforth†, J P Kotthaus†, C R Bolognesi‡, C Nguyen‡§, B Brar‡ and H Kroemer‡

† Sektion Physik der LMU München, D-80539 München, Germany
‡ Department of Electrical and Computer Engineering, UC Santa Barbara, CA 93106, USA

Abstract. The influence of conduction band non-parabolicity on the cyclotron resonance of a two-dimensional electron system in InAs quantum wells is investigated. We demonstrate that the experimentally determined dependence of the cyclotron mass on the carrier density in the well can be excellently described using a two-band $k \cdot p$ model. In contrast to previously studied systems our experimental results allow us to deduce quantitatively the quantization energy of the first electrical subband for wells of different width.

Much effort is devoted in semiconductor science to tailor new band structures in order to optimize device performance. InAs/AlSb quantum wells grown on GaAs substrates have a band line-up differing substantially from the widely studied GaAs/AlGaAs system and can therefore be expected to complement GaAs/AlGaAs-based devices. The narrow-bandgap semiconductor InAs (E_g = 0.4 eV) is sandwiched between AlSb barriers (E_g, Γ = 2.3 eV) leading to a type II staggered structure [1]. The resulting conduction band quantum well is approximately 2.1 eV deep at the Γ point and makes possible extremely large electronic quantization energies when the well is sufficiently narrow. Moreover, the low InAs conduction band edge mass ($m_\Gamma^*/m_0 \approx 0.023$) results in very large subband separations in the wells. Despite a lattice mismatch between the GaAs substrate and the InAs well of approximately 7%, low-temperature mobilities can reach values as high as 800 000 $cm^2\ V^{-1}\ s^{-1}$ [2]. Several devices made of InAs quantum wells have already been demonstrated, for instance resonant tunnelling diodes [3] with extraordinarily high peak-to-valley ratios and transistors [4]. The small effective InAs electron mass leads to large optical matrix elements making the material attractive for detectors and modulators working in the mid and near infrared. To optimize all these possible devices a detailed knowledge of the material's characteristics is a highly desired prerequisite.

In this paper, we present cyclotron resonance measurements on InAs/AlSb wells of different widths and carrier densities. Our results clarify the influence of the conduction band non-parabolicity on the subband structure as well as on the density of states of the InAs wells. Four samples A, B, C, D consisting of the following layer sequence were investigated. On the GaAs substrate a 1–2 μm AlSb buffer was grown followed by a 10-period superlattice as described elsewhere [5]. On top of that the InAs well (15 nm wide for samples A, B and 12 nm wide for samples C, D) was sandwiched between 20 nm AlSb barriers. All samples were capped with a 5 nm layer of GaSb to prevent the AlSb from oxidizing when exposed to air.

The far-infrared spectra were taken using a rapid-scan Fourier transform spectrometer with the samples mounted in a superconducting solenoid. All experiments were performed at low temperatures $T \approx 2$ K. Experimentally, we determined the relative change in far-infrared (FIR) transmission with and without a perpendicular magnetic field $T(B \neq 0)/T(B = 0)$ where the field strength was kept low in order to ensure $\hbar\omega_c \ll E_F$. The carrier density N_s in the wells was tuned by taking advantage of the persistent photoeffects present in the samples. In the spectral range between $h\nu$ = 1.0 eV and $h\nu$ = 3.0 eV both negative as well as positive persistent photoeffects were observed [6], allowing for a reproducible control of the carrier density in the wells. We used an optical fibre to focus the visible radiation onto the sample.

In figure 1 we show a set of typical cyclotron resonance (CR) spectra. We plot the relative change in FIR transmission at a fixed magnetic field of B = 2 T for different illumination wavelengths. To ensure saturation of the photoeffects, all spectra are taken under continuous illumination. As stated above, the energy of the illuminating light determines the carrier density such that the different traces correspond to different well fillings. Experimentally, we determine the electron

§ Now at Hughes Research Laboratories Malibu, CA 90265, USA.

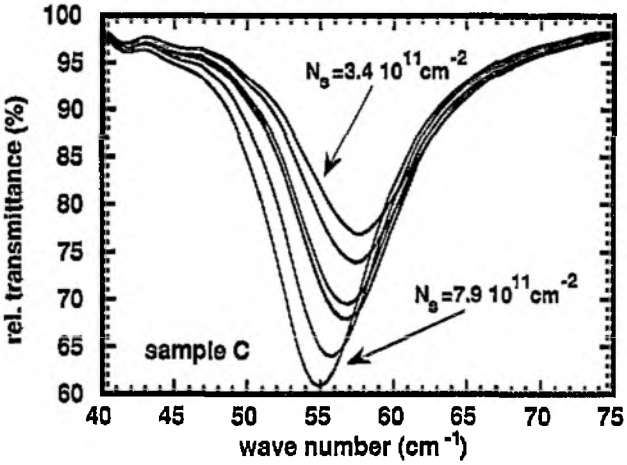

Figure 1. Relative transmission spectra of sample C taken for different carrier densities N_s at $B = 2$ T. As the electron concentration in the well increases (larger area under the resonance traces) the resonance position shifts to lower energies corresponding to a higher effective mass.

concentration N_s from the oscillator strength of the resonance while the cyclotron mass is given by the resonance energy. Clearly, a strong dependence of both the oscillator strength and the resonance position of the CR is observed in the figure. With increasing illumination energy $h\nu$ the oscillator strength decreases, indicating a decreasing carrier density in the well. At the same time the resonance shifts to higher energies, i.e. the cyclotron mass $m_c = eB/\omega_{res}$ decreases with decreasing N_s. In general terms, this behaviour is well known for non-parabolic semiconductors and has been discussed before in great detail [7].

However, it would be highly desirable to obtain a quantitative picture of the situation for a strongly non-parabolic quantum well system like, for example, InAs, since here only a very accurate description of the non-parabolic dispersion is expected to result in a proper agreement with the experimental observations. GaAs is not a suitable material for such studies since it is only slightly non-parabolic and the necessary inclusion of higher conduction bands to describe the dispersion relation accurately makes the analysis rather cumbersome. On the other hand, InSb is strongly non-parabolic but there are no high-quality quantum wells of this material available to date. The triangular potential so far realized on InSb MOS devices is not an appropriate choice either: firstly, the quantization energies are quite low in comparison with the Fermi energy and therefore have a small influence on the cyclotron mass. Because of the low subband energies even moderately high carrier densities invariably lead to the occupation of a second subband which hampers the study of the energy-dependent density of states in the lowest subband (electric quantum limit). Secondly, a variation of the electron concentration results in a self-consistent change of the confining potential that makes it difficult to analyse non-parabolicity effects on InSb MOS capacitors [8]. In order to investigate quantitatively the effect of non-parabolicity on a 2DEG one needs a strongly non-parabolic electron system confined by an external potential so high that self-consistent effects resulting from occupation with electrons can be treated perturbatively. As we will show, InAs/AlSb is a material combination well suited to fulfil these requirements.

To interpret our data we derive the cyclotron mass from the two-band dispersion relation

$$E(E + E_g) = E_g \frac{\hbar^2(k_\parallel^2 + k_\perp^2)}{2m_0}. \tag{1}$$

Here, $k_\parallel$ denotes the wavevector in the plane of the quantum well while $k_\perp$ is the wavevector perpendicular to the well. The zero of the energy scale is taken to be at the bottom of the InAs conduction band. $E_g = 0.42$ eV is the low-temperature bandgap energy [9]. The other symbols have their usual meaning. Quantizing $k_\perp$ in the effective mass approximation (EMA), i.e. assuming parabolic bands, gives the subband energy E_0^{EMA}. In the framework of the two-band model the electron energy E reads

$$E = -\frac{E_g}{2} + \sqrt{\frac{E_g^2}{4} + E_g E_0^{EMA} + E_g \frac{\hbar^2 k_\parallel^2}{2m_0^*}}. \tag{2}$$

It is clear from (2) that the electron energy E is not simply given by the sum of the subband energy E_0 and the kinetic energy $E_\parallel$ [10]. In narrow-gap semiconductors the motion parallel and perpendicular to the two-dimensional electron gas couple. The physical reason for this coupling is the strong interaction between conduction and valence bands for small values of the energy gap E_g. Experimentally, this coupling has been observed as a violation of the polarization selection rule for intersubband transitions [11]. It is only in the limit of $E_g \gg E_0, E_\parallel$ that the energies E_0 and $E_\parallel$ can simply be added to give the electron energy E.

In the semiclassical approach the Fermi velocity is given by

$$v_F = \frac{1}{\hbar}\frac{\partial E}{\partial k_\parallel} = \frac{E_g}{E_g + 2E}\frac{\hbar k_{\parallel F}}{m_0^*} \tag{3}$$

which leads via the Lorentz force law $\hbar\dot{k} = e v_F B$ to the relation for the cyclotron resonance frequency

$$\omega_c = 2\pi\frac{\dot{k}}{2\pi k_{\parallel F}} = \frac{E_g}{E_g + 2E}\frac{eB}{m_0^*} = \frac{eB}{m_c^*} \tag{4}$$

where

$$m_c^* = \frac{E_g + 2E}{E_g} m_0^* \tag{5}$$

is the cyclotron resonance effective mass. Here E is given by (2).

The above equations allow us to obtain an analytical expression for the dependence of the cyclotron mass on the carrier density with the energy of the first subband E_0^{EMA} being the only fit parameter

$$m_c^* = \frac{2m_0^*}{E_g}\sqrt{\frac{E_g^2}{4} + E_g E_0^{EMA} + E_g \frac{\pi\hbar^2 N_s}{m_0^*}}. \tag{6}$$

According to (6) the subband energy E_0^{EMA} determines the slope of the m_c versus N_s curve as well as the value $m_c(N_s) = 0$. As in the experimental data, high subband energies as expected for narrow wells lead to larger values $m_c(N_s = 0)$ and to a weaker dependence of the cyclotron mass m_c on the carrier density N_s.

It can be shown quite generally that the energy-dependent density of states mass m_D^* defined by

$$D(E) = \frac{m_D^*}{\pi\hbar^2} \tag{7}$$

is identical to the cyclotron mass, i.e. within the framework of a two-band model m_D^* is also given by (6).

A critical measure of the validity of the above model is the degree to which it gives a correct description of the $m_c(N_s)$ dependence, i.e. the non-parabolic density of states. We find that the data can be described excellently by the two-band model up to carrier densities as high as 1.3×10^{12} cm^{-2} (figure 2). We obtain ground state subband energies of E_0^{EMA} (12 nm) = 96 meV and E_0^{EMA} (15 nm) = 58 meV from the best fit. These values can be compared with the ground state subband energies E_0^{np} that are deduced in the two-band model (1) taking non-parabolicity and $k_\parallel = 0$ into account

$$E_0^{EMA} = E_0^{np}\left(1 + \frac{E_0^{np}}{E_g}\right). \tag{8}$$

The results are E_0^{np} (12 nm) = 81 meV and E_0^{np} (15 nm) = 52 meV which are in very good agreement with values derived previously [12–14]. Thus the measurement of the carrier-density-dependent cyclotron mass allows us to derive the absolute value of the ground state energy at $N_s = 0$. Intersubband transition and interband transition experiments, on the other hand, reveal the energetic difference between two energy levels. Intersubband absorption measurements on 15 nm wide InAs/AlSb quantum wells [15] give subband spacings of approximately 100 meV which is also in good agreement with multiband calculations [12–14]. Combining the different methods one can thus test the theoretical predictions of the energy ladder in InAs/AlSb quantum wells experimentally.

Our data can be interpreted in such a straightforward way only because for InAs/AlSb quantum wells the self-consistent band bending has, to a first approximation, no effect on the cyclotron mass. This is because the quantum well barrier is 2.1 eV high at the Γ point so that the external potential is essentially independent of the carrier density. It can be shown that for such deep potential wells first-order perturbation theory gives subband energies which hardly deviate from the self-consistent result up to electron concentrations as high as in our experiments. This means that as long as first-order perturbation theory describes the subband energies sufficiently accurately the self-consistent potential does not influence the energy-dependent cyclotron mass.

In [16] it is claimed that the cyclotron mass should depend sensitively on the strain present in the structure.

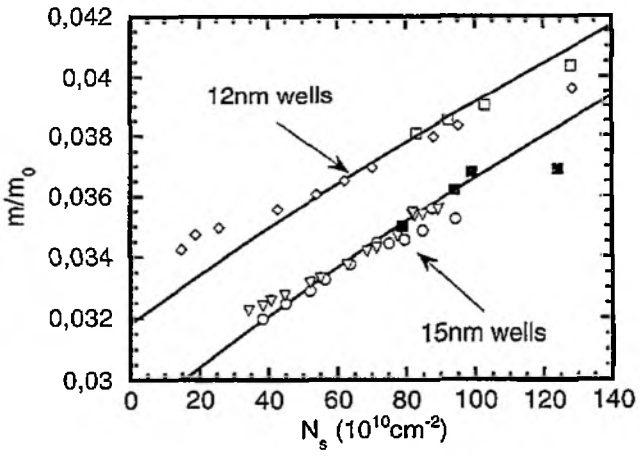

Figure 2. The best fit of the data to the theoretical $m_c^*(N_s)$ curve. The only fit parameter is the subband energy. Samples A, B and C, D are denoted by the open symbols. The full squares show cyclotron masses of four different 15 nm wide quantum wells grown on GaSb buffers. The $m_c^*(N_s)$ dependence of the data can be well described by the very same parameters used for quantum wells grown on AlSb buffers.

In InAs/AlSb the strain results from the lattice mismatch between the pseudomorphically grown InAs well and the buffer layers. To clarify this point we have measured the cyclotron resonance also on four different samples grown not on AlSb buffers ($e_{xx} = 1.27\%$) but on GaSb buffers ($e_{xx} = 0.62\%$). These samples are otherwise almost identical to the ones grown on AlSb buffers described above. As shown in figure 2 there is no systematic deviation of the cyclotron mass when comparing the two sets of samples. This leads us to conclude that the strain dependence of the cyclotron mass caused by different buffer layers is but very little in our samples and can therefore be neglected.

In summary, we have shown that a simple two-band model describes the electron dispersion in InAs/AlSb quantum wells very accurately provided that non-parabolicity effects are properly taken into account. The analysis is greatly facilitated by the fact that for such high external potentials as in InAs wells self-consistent effects can be neglected. We derive absolute values of the ground state energies for wells with $N_s = 0$ from our experiments that are in good agreement with theoretical models based on a multiband approach.

Acknowledgments

The work in Munich was sponsored by the Volkswagen Stiftung. The Santa Barbara group gratefully acknowledges support from the Office of Naval Research and from QUEST, the NSF Science and Technology Center for Quantized Electronic Structures (grant DMR 91-20007).

References

[1] Tuttle G, Kroemer H and English J H 1989 *J. Appl. Phys.* 65 5239

[2] Nguyen G 1993 *Dissertation* UC Santa Barbara
[3] Chen J F, Wu M C, Yang L and Cho A Y 1990 *J. Appl. Phys.* **68** 3040
[4] Bolognesi C R, Caine E J and Kroemer H 1993 *IEEE Trans. Electron. Devices* **40** 2114
[5] Tuttle G, Kroemer H and English J H 1990 *J. Appl. Phys.* **67** 3032
[6] Gauer C, Scriba J, Wixforth A, Kotthaus J P, Nguyen C, Tuttle G, English J H and Kromer H 1993 *Semicond. Sci. Technol.* **8** S137
[7] See, for example, Merkt U 1987 *Festkörperprobleme* ed P Grosse (Braunschweig: Vieweg) pp 109–36
[8] Merkt U, Horst M, Evelbauer T and Kotthaus J P 1986 *Phys. Rev.* B **34** 7234
[9] Madelung O (ed) 1982 *Landolt-Börnstein, Numerical Data and Functional Relationships in Science and Technology, New Series* vol 17 (Berlin: Springer)
[10] Zawadzki W 1983 *J. Phys. C: Solid State Phys.* **16** 229
[11] Wiesinger K, Reisinger H and Koch F 1982 *Surf. Sci.* **113** 102
[12] Bastard G 1982 *Phys. Rev.* B **48** 7584
[13] White S R and Sham L J 1981 *Phys. Rev. Lett.* **47** 879
[14] Taylor R I and Burt M G 1987 *Semicond. Sci. Technol.* **2** 485
[15] Simon A, Scriba J, Gauer C, Wixforth A, Kotthaus J P, Bolognesi C R, Nguyen C, Tuttle G and Kroemer H. 1993 *Mater. Sci. Eng.* B **21** 201
[16] Lin-Chung P J and Yang M J 1993 *Phys. Rev.* B **48** 5338